Heat Transfer 1982
Proceedings of the Seventh International Heat Transfer Conference
Munchen, Fed. Rep. of Germany, Vol. 2

A THEORETICALLY BASED CORRELATION FOR NATURAL CONVECTION IN HORIZONTAL RECTANGULAR ENCLOSURES HEATED FROM BELOW WITH ARBITRARY ASPECT RATIOS

Hiroyuki Ozoe [1]
Keiichi Fujii [1]

Stuart W. Churchill [2]
Noam Lior [2]

[1] Okayama University, Tsushima, Okayama, 700 Japan
[2] University of Pennsylvania, Philadelphia, Pennsylvania 19104, U.S.A.

ABSTRACT

New theoretical results are presented from which the overall Nusselt number for natural convection can be compiled for a rectangular enclosure of arbitrary dimensions, heated from below. This procedure is applicable for all aspect ratios greater than unity and for Rayleigh numbers up to at least 20,000. The solutions were obtained by a finite-difference method, using a three-dimensional model for (1) long roll cells with a square cross-section, free-free and rigid-free lateral boundaries, and rigid-rigid end and horizontal boundaries; and (2) cubical roll cells with a complete set of vertical boundary conditions. The numerical solutions were extrapolated to zero grid-size. The predicted Nusselt numbers are in good agreement with prior experimental data for various Ra, Pr and aspect ratios, including the limiting case of infinite parallel plates.

1. INTRODUCTION

The critical Rayleigh number for natural convection in rectangular boxes heated from below and cooled from above has been determined theoretically by Davis [1] and Catton [2], and an expression for the rate of heat transfer in an infinite fluid layer with Ra somewhat greater than Ra_c has been derived by Malkus and Veronis [3]. However, generalized theoretical or empirical expressions do not appear to have been developed for the rate of convective heat transfer in rectangular boxes of arbitrary dimensions. This paper presents approximate theoretical results from which such behavior can be predicted without empiricism.

2. PHYSICAL MODEL

The circulation pattern is postulated to consist of an integral number of equally sized, long roll cells whose axes are parallel to the shorter horizontal dimension of the enclosure. The dimensions of rolls are postulated to be ℓH, H and H in the x, y and z directions, respectively. The total number of rolls in the y-direction is m. The rolls adjacent to y=0 and y=mH have one rigid and one free vertical lateral boundary. The internal rolls have two free vertical lateral boundaries. Figures 1 and 2 show schematics of these two types of rolls in dimensional and dimensionless coordinates, respectively. m is necessarily greater than ℓ to assure that the axes of the rolls are parallel to the shorter horizontal dimension of the enclosure. Both of these types of roll cells are three-dimensional owing to the rigid vertical walls at the ends of the rolls (X=0 and ℓ).

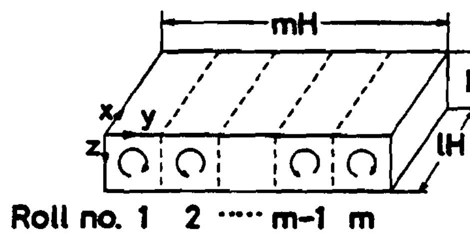

Figure 1 The m long roll cells in a rectangular box heated from below, cooled from above and thermally insulated on the four vertical walls.

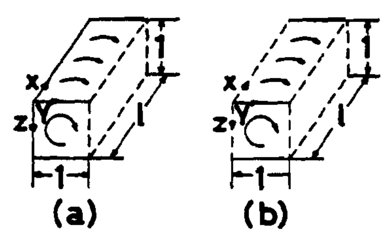

Figure 2 Two types of a long roll cell (a) R-F (rigid boundary wall at Y=0 and free boundary at Y=1) (b) F-F (free boundary at Y=0,1).

This general mode of circulation has a firm experimental basis. However, as discussed in detail by Ozoe et al. [4], the cell width-to-height ratio in low-Prandtl-number fluids has been observed and computed by prior investigators to increase continuously above unity in an infinite layer, and discretely in a finite rectangular enclosure, as the Rayleigh number increases above the critical value. On the other hand, the cell width does not appear to increase in large-Prandtl-number fluids. Furthermore, the average

Nusselt number, as obtained from their finite-difference computations, does not vary significantly with the postulated width-to-height ratio of the cell. The postulate of an integral number of roll cells of square section is therefore presumed to introduce negligible error in Nu for the low-Rayleigh-number range of this investigation, even for the limiting case of an infinite layer.

3. MATHEMATICAL MODEL

The equations describing natural convection in a long roll cell have previously been derived by Ozoe, et al. [5]. They can be reduced to the following dimensionless expressions for the conservation of energy and vorticity:

$$\frac{D\phi}{D\tau} = \nabla^2\phi \tag{1}$$

and

$$\frac{D\vec{\Omega}}{D\tau} - (\vec{\Omega}\cdot\nabla\vec{V}) = Pr\,\nabla^2\vec{\Omega} + Ra\,Pr\begin{pmatrix}-\partial\phi/\partial Y\\ \partial\phi/\partial X\\ 0\end{pmatrix} \tag{2}$$

where

$$\vec{\Omega} = \nabla\times\vec{V} = -\nabla^2\vec{\Psi} \tag{3}$$

and

$$\nabla\cdot\vec{\Psi} = 0 \tag{4}$$

The corresponding boundary conditions for a single long roll are:

at $X = 0,\ \ell$

$$\frac{\partial\Psi_1}{\partial X} = \Psi_2 = \Psi_3 = U = V = W = \frac{\partial\phi}{\partial X} = \Omega_1 = 0,\quad \Omega_2 = -\frac{\partial W}{\partial X},\ \Omega_3 = \frac{\partial V}{\partial X} \tag{5}$$

at $Z = 0,\ 1$

$$\Psi_1 = \Psi_2 = \frac{\partial\Psi_3}{\partial Z} = U = V = W = \Omega_3 = 0,\quad \Omega_1 = -\frac{\partial V}{\partial Z},\ \Omega_2 = \frac{\partial U}{\partial Z},\ \phi = \mp 0.5 \tag{6}$$

at $Y = 0$ for a rigid boundary

$$\Psi_1 = \frac{\partial\psi_2}{\partial Y} = \Psi_3 = U = V = W = \frac{\partial\phi}{\partial Y} = \Omega_2 = 0,\quad \Omega_1 = \frac{\partial W}{\partial Y},\ \Omega_3 = -\frac{\partial U}{\partial Y} \tag{7}$$

and at $Y = 0,\ 1$ for dragless boundaries

$$\Psi_1 = \frac{\partial\Psi_2}{\partial Y} = \Psi_3 = \frac{\partial U}{\partial Y} = V = \frac{\partial W}{\partial Y} = \Omega_1 = \Omega_3 = \frac{\partial\phi}{\partial Y} = \frac{\partial\Omega_2}{\partial Y} = 0 \tag{8}$$

4. NUMERICAL SCHEME

The central-difference and alternating-direction-implicit (ADI) method described by Ozoe, et al. [4] was used. The dimensionless time step was 0.001. For $\ell = 1, 2$; $\Delta X = \Delta Y = \Delta Z = 0.1$. For $\ell \geq 3$, a varying ΔX was used as defined below. (The number of grid points in the X-direction was limited to 21 by the computer memory.)

$$X_i = \frac{1}{a}\left(e^{\bar{X}_i/b} - 1\right) \text{ for } \bar{X}_i = 0 \sim \frac{\ell}{2} \tag{9}$$

$$X_i = \frac{1}{a}\left(1 + a\ell - e^{(\ell - \bar{X}_i)/a}\right) \text{ for } \frac{\ell}{2} < \bar{X}_i < \ell \tag{10}$$

$$\bar{X}_i = \frac{\ell}{20},\ \frac{2\ell}{20}\ldots\ell$$

$$\left.\begin{matrix}a = 0.8732\\ b = 1.7918\end{matrix}\right)_{\ell=3};\quad \left.\begin{matrix}a = 1.469\\ b = 1.459\end{matrix}\right)_{\ell=4};$$

$$\left.\begin{matrix}a = 47.39\\ b = 0.2578\end{matrix}\right)_{\ell=7}$$

5. NUMERICAL RESULTS

Finite-difference computations are subject to truncation error. To minimize this error, the Nusselt number at zero grid size was estimated by extrapolation, as described by Churchill, et al. [6], assuming a second-order local discretization error.

For the case of a 2x1x1 roll cell with free lateral vertical boundaries, three-dimensional computations were carried out for Ra=3000, 4000, 6000 and 20000 for both ΔZ=1/10 and ΔZ=1/14. The results are listed in Table 1. The expression $Nu = a' + b'(\Delta Z)^2$ was then used to obtain the listed Nusselt numbers for $\Delta Z \to 0$. These values for $\Delta Z \to 0$ are plotted versus the Nusselt number at $\Delta Z = 0.1$ in Fig. 3. This curve is expected to be applicable for other Rayleigh numbers, aspect ratios and vertical boundary conditions, since the Nusselt number is affected primarily by the grid size in the vertical direction (the heat flux is calculated from the temperature gradient in that direction). The Nusselt numbers for other conditions were obtained from calculations at Z=0.1, and Fig. 3.

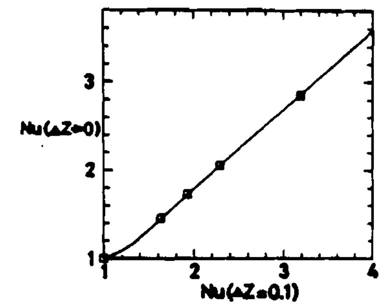

Figure 3 Reference curve giving the Nusselt number at zero grid size from the Nusselt number computed at ΔZ=0.1. (2x1x1 F-F roll cell at Ra=3000, 4000, 6000 and 20000, Pr=10).

The effect of the length of the roll in the axial direction was investigated for Ra=4000 and Pr=10 for both free-free and rigid-free conditions. The computed Nusselt numbers for ΔZ=0.1 and the estimated values for ΔZ→0 are listed in Table 2. The values for ΔZ→0 are seen in Fig. 4 to vary linearly with the inverse of the roll length ($1/\ell$), over the entire range of ℓ from 1 to ∞. At Ra=4000, with free-free boundaries:

$Nu = 1.908 - 0.377/\ell$

At Ra = 4000 with rigid-free boundaries:

$Nu = 1.642 - 0.332/\ell$

Such linear relationships are expected to hold for other Rayleigh numbers.

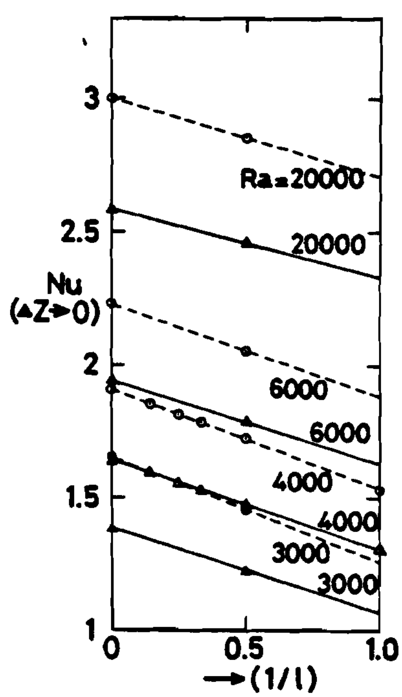

Figure 4 Dependence of the Nusselt number of a roll cell on the inverse of aspect ratio.

———————— R-F - - - - - - - - - - - F-F

Computations were also carried out for Ra=3000, 6000 and 20000 for ∞x1x1 and 2x1x1 roll cells with both free-free and rigid-free boundaries. The Nusselt numbers obtained by extrapolation to zero grid size are listed in Table 3. The constants in the linear equations

$$Nu_{RF} = a - \frac{b}{\ell} \qquad (11)$$

and

$$Nu_{FF} = c - \frac{d}{\ell} \qquad (12)$$

are listed in Table 4 and plotted vs. the Rayleigh number in Fig. 5.

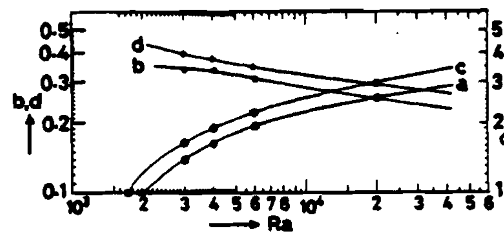

Figure 5 Dependence of coefficients a, b, c and d on the Rayleigh number.

0, +, • Computed Results

□ Critical Rayleigh number for infinite layer

△ Critical Rayleigh number computed by Catton [2] for a 12x2x1 enclosure.

6. ILLUSTRATIVE APPLICATION

Consider a 7x10x1 enclosure at Ra=4000. From Fig. 5, c=1.908, d=0.377 and Nu_{FF}=1.908-0.377/7 = 1.8541. Similarly, Nu_{RF}= 1.642-0.332/7 = 1.5946. Ten rolls are postulated to occur, two of them are rigid-free and 8 are free-free. The average Nusselt number is accordingly

$$Nu_{7x10x1} = \frac{2(1.5946) + (10-2)(1.8541)}{10} = 1.802$$

7. COMPARISON WITH PRIOR RESULTS

7.1 Infinite Layer of Fluid

The constant c corresponds to the Nusselt number for an infinite layer of fluid between horizontal plates. This value, as obtained from Fig. 5, is compared in Fig. 6 with the experimental data of Silveston [7] and with the following theoretical expression of Malkus and Veronis [3]:

$$Nu = 1 + 1.446\left(1 - \frac{1708}{Ra}\right) S\{1708\} + 1.664\left(1 - \frac{17610}{Ra}\right) S\{17610\} \qquad (13)$$

The values computed herein appear to be an upper bound for the experimental data whereas Equation (13) is a lower bound.

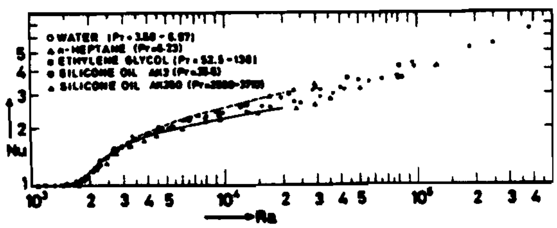

Figure 6 Comparison of the computed values of the Nusselt number for an infinite layer with the experimental data of Silveston [8]
-----this work (Pr=10),
———Equation (13), Malkus and Veronis [3].

7.2 Finite Rectangular Enclosures

The predictions of the mean Nusselt number by the above procedure are compared in Table 5 with the experimental values of Ozoe, et al. [8, 9] for a wide range of aspect ratios and Rayleigh numbers. The values of the coefficients a, b, c, and d read from Fig. 5, and the corresponding values of Nu_{RF} and Nu_{FF} computed from Equations (11) and (12) are included in the table. The experimental values would be anticipated to be somewhat higher due to finite conduction in the Plexiglas side walls. The computations and correlation are for Pr=10, which is presumed to be asymptotically large. Hence no discrepancy on this account would be expected for the experiments with silicone oil (Pr>4000), but the predictions would be expected to be slightly low for the indicated experiments with air. Considering these factors and the scatter in the data, the agreement is judged to be very good.

8. TEST OF USE OF NON-UNIFORM GRID SPACING

As noted above, numerical calculations for ℓ greater than 2 were carried out for a non-uniform grid spacing in the X-direction. To check the effect of the non-uniform grid spacing, the following test was made. The long roll cells shown in Fig. 1, were considered to be divided into a number of cubic volumes and classified on the basis of the vertical boundary conditions, as shown in Fig. 7. Suppose ℓ is an integer, then Roll No. 1, which has a rigid vertical boundary on the left side and a free boundary on the right side, can be subdivided into ℓ cubes, two of Type A and the balance of Type B. Type A is a corner cube with rigid vertical boundaries at X=0 and Y=0. Type B has one rigid vertical boundary at Y=0. Roll No. 2 which has free-free vertical lateral boundaries, can similarly be divided into cubes of the C and D types. Type C has one rigid vertical boundary at X=0. Type D has no rigid vertical boundaries. Type E (not shown), which occurs only in a 1xmx1 box, has three rigid vertical boundaries and one free at Y=1. Type F (not shown), which occurs only for a cubic box, has four rigid vertical boundaries. Calculations for these six cubes were carried out for Ra=4000 and $\Delta X=\Delta Y=\Delta Z=0.1$. The results, together with values extrapolated to zero grid-size per Fig. 3, are in Table 6. The extrapolated values can be used to compute values for long roll cells. For example a 7x1x1 roll cell can be divided into two C rolls and five D rolls. The average Nusselt number, using the values in Table 6 is then

$$Nu_{7x1x1} = \frac{2Nu_C + 5Nu_D}{7} = \frac{2x1.723 + 5x1.908}{7} = 1.855$$

The values obtained in this way are compared in Table 2 with the previously calculated values for long roll cells. The agreement is excellent, providing a further confirmation of the validity of using a non-uniform grid spacing in the x-direction.

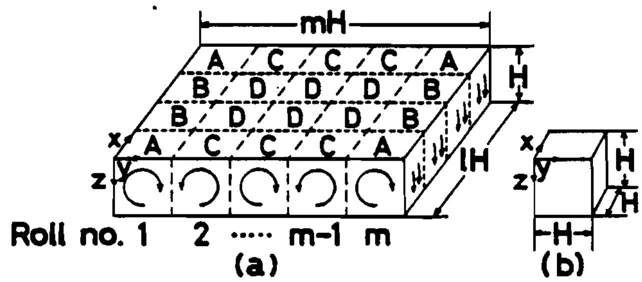

Figure 7 Cubical regimes in a rectangular box.
(a) ℓHxmHxH box
(b) coordinates of a cubical regime.

9. ALTERNATIVE CORRELATION

The above agreement suggest that the Nusselt number for any rectangular enclosure, even with non-integer values of ℓ can be estimated for Ra=4000 using the values in Table 6. Values equivalent to those in Table 6 could be estimated for other Rayleigh numbers using Fig. 5 and Equations (11) and (12). However the direct use of Fig. 5 and these equations is more convenient.

The agreement between these two computational procedures indicates that the effect of the rigid end wall does not extend more than the distance H.

10. SUMMARY OF CORRELATION

1. Read a, b, c and d from Fig. 5 for the specified Rayleigh number.
2. Calculate ℓ=short horizontal dimension/height.
3. Calculate Nu_{RF} and Nu_{FF} from Equations (11) and (12).
4. Calculate m=long horizontal dimensions/height.
5. Calculate Nu from

$$Nu = \frac{2Nu_{RF} + (m-2)Nu_{FF}}{m}$$

11. SUMMARY AND CONCLUSIONS

A theoretically based procedure has been developed to predict the average Nusselt number for a rectangular enclosure heated from below, cooled from above and thermally insulated on the four surrounding vertical walls.

The predictions are in good agreement with experimental data for air, water, glycol and oils over a wide range of aspect ratios.

This correlation is based on exact solutions at $Ra=3\times10^3-2\times10^4$ and $Pr=10$ for $\ell\times1\times1$ roll cells with the two possible boundary conditions. This extension of prior theoretical work for $2\leq\ell<\infty$ is based on the use of the staggered grid described in reference [4] and on an extrapolation to zero grid size which is validated in reference [6].

The solutions are approximations for the behavior in rectangular enclosures in that the width-to-height ratio of roll cells is known to increase above unity as the Rayleigh number increases above the critical value, and to be less near the side walls than at the center. However, the error in the overall Nusselt number due to this postulate is shown in reference [4] to be negligible, at least for $Ra<20000$.

The method of prediction introduces no empiricism, per se, but linear and graphical interpolation, respectively, are required for length-to-height ratios and Rayleigh numbers intermediate to those of the calculations herein.

The correlation appears to be a good approximation for all $Pr\geq0.7$ and for aspect ratios greater than unity.

An equivalent but less convenient correlation was also developed on the basis of the computed motion in cubical regions with a complete set of boundary conditions.

ACKNOWLEDGEMENT

The computations were carried out at the Okayama University Computer Center. This work was supported in part by a Grant in Aid for Scientific Research on Special Research Projects on Energy Problems from the Ministry of Education, Japan (No. 56040063).

NOMENCLATURE

- A — type of cubical region
- B — type of cubical region
- C — type of cubical region
- c — constant = Nusselt number $\ell=m=\infty$
- D — type of cubical region
- g — acceleration due to gravity, m/s^2
- H — height of a rectangular box, m
- ℓ — smaller aspect ratio
- m — larger aspect ratio
- Nu — Nusselt number = $qH/\lambda(T_h-T_c)$
- Pr — Prandtl number = ν/α
- q — heat flux density, W/m
- Ra — Rayleigh number = $g\gamma(T_h-T_c)H^3/\alpha\nu$
- $S\{Ra_i\}$ — step function: 0 for $Ra<Ra_i$; 1 for $Ra>Ra_i$
- T — temperature, K
- T_c — temperature, of cold plate, K
- T_h — temperature, of hot plate, K
- T_o — mean temperature = $(T_c+T_h)/2$, K
- t — time, s
- u — velocity component in x-direction, m/s
- U — dimensionless velocity component = uH/α
- v — velocity component in y-direction, m/s
- V — dimensionless velocity component = vH/α
- w — velocity component in z-direction, m/s
- W — Dimensionless velocity component = wH/α
- x — distance along roll cell, m
- X — dimensionless coordinate = x/H
- y — distance across roll cell, m
- Y — dimensionless coordinate = y/H
- z — downward vertical distance, m
- Z — dimensionless coordinate = z/H
- α — thermal diffusivity, m/s
- γ — volumetric coefficient of expansion, K^{-1}
- λ — thermal conductivity, W/mK

REFERENCES

1. Davis, S.H., Convection in a Box: Linear Theory, J. Fluid Mech., vol. 30, pp. 465-478, 1967.

2. Catton, I., The Effect of Insulating Vertical Walls on the Onset of Motion in a Fluid Heated from Below, Int. J. Heat Mass Transfer, vol. 15, pp. 665-672, 1972.

3. Malkus, W.V.R., and Veronis, G., Finite Amplitude Cellular Convection, J. Fluid Mech., vol. 4, pp. 225-260, 1958.

4. Ozoe, H., Fujii, K., Lior, N., and Churchill, S. W., Long Rolls Generated by Natural Convection in an Inclined Rectangular Enclosure, (in review).

5. Ozoe, H., Yamamoto, K., Sayama, H., and Churchill, S.W. S. W., Natural Convection Patterns in a Long Inclined Rectangular Box Heated from Below, Int. J. Heat Mass Transfer, vol. 20, pp. 131-139, 1977.

6. Churchill, S. W., Chao, P., and Ozoe, H., Extrapolation of Finite-Difference Calculations of Laminar Natural Convection in Enclosures to Zero Grid Size, Numerical Heat Transfer, vol. 4, pp. 39-51, 1981.

7. Silveston, P. L., Wärmedurchgang in waagerechtin Flüssigkeitsschichten, Forsch. Ing-Wes., vol 4, pp. 59-69, 1958.

8. Ozoe, H., Sayama, H., and Churchill, S.W., Natural Convection in an Inclined Square Channel, Int. J. Heat Mass Transfer, vol. 17, pp. 401-406, 1974.

9. Ozoe, H., Sayama, H., and Churchill, S. W., Natural Convection in an Inclined Rectangular Channel at Various Aspect Ratios and Angles-Experimental Measurements, Int. J. Heat Mass Transfer, vol. 18, pp. 1425-1431, 1975.

Table 1 Computed and extrapolated results for 2x1x1, free-free roll cells at Pr=10.

Ra \ ΔZ	Nusselt number 1/10	1/14	ΔZ→0
3000	1.6326	1.5445	1.4528
4000	1.9242	1.8253	1.7223
6000	2.2835	2.1725	2.0570
20000	3.1872	3.0234	2.8530

Table 2 Computed Nusselt numbers for long roll cells, with rigid-free and free-free boundaries, at Ra=4000 and Pr=10.

	R-F		F-F		Synthesized from cubes	
ℓx1x1	ΔZ=0.1	ΔZ→0	ΔZ=0.1	ΔZ→0	R-F (ΔZ→0)	F-F (ΔZ→0)
1x1x1	1.4607	1.300	1.719	1.531		
2x1x1	1.655	1.476	1.924	1.722	$\frac{A+A}{2}=1.473$	$\frac{C+C}{2}=1.723$
3x1x1	1.715	1.528	1.990	1.782	$\frac{2A+B}{3}=1.529$	$\frac{2C+D}{3}=1.785$
4x1x1	1.746	1.557	2.023	1.813	$\frac{2A+2B}{4}=1.558$	$\frac{2C+2D}{4}=1.815$
7x1x1	1.785	1.592	2.066	1.853	$\frac{2A+5B}{7}=1.594$	$\frac{2C+5D}{7}=1.855$
∞x1x1	1.839	1.642	2.124	1.908	B=1.642	D=1.908

Table 3 Computed and extrapolated Nusselt numbers of roll cells for different Rayleigh numbers, boundary conditions and aspect ratios (Pr=10).

lateral vertical boundaries	roll cell size	Ra 3000 ΔZ=0.1	ΔZ→0	4000 ΔZ=0.1	ΔZ→0	6000 ΔZ=0.1	ΔZ→0	20000 ΔZ=0.1	ΔZ→0
R-F	2x1x1	1.371	1.220	1.655	1.476	2.000	1.788	2.738	2.458
	∞x1x1	1.557	1.386	1.839	1.642	2.161	1.943	2.882	2.585
F-F	2x1x1	1.633	1.453	1.924	1.723	2.284	2.057	3.187	2.853
	∞x1x1	1.849	1.650	2.124	1.908	2.462	2.230	3.371	3.000

Table 4 Dependence of parameters for roll cells on Rayleigh number (Pr=10).

constants \ Ra	3000	4000	6000	20000
a	1.386	1.642	1.943	2.585
b	0.332	0.332	0.31	0.254
c	1.650	1.908	2.230	3.000
d	0.394	0.377	0.346	0.294

Table 5 Comparison of Predicted and Measured Values of Overall Nusselt Number[a]

W/H	L/H	Ra	a	b	c	d	Nu_{RF}	Nu_{FF}	$Nu_{pred.}$	$Nu_{exp.}$	%Error
1	18	11000	2.3	0.27	2.63	0.318	2.03	2.312	2.28	2.49[b]	- 8.4
		4950	1.88	0.32	2.1	0.353	1.56	1.747	1.726	1.7[b]	+ 1.5
		3800	1.63	0.336	1.9	0.38	1.294	1.52	1.495	1.45[b]	+ 3.1
1.88	11.23	10300	2.22	0.282	2.6	0.32	2.07	2.43	2.366	2.67	-11.4
3.03	12.12	20000	2.5	0.26	3.0	0.3	2.414	2.9	2.82	2.88	- 2.8
4.22	12.63	16800	2.42	0.262	2.86	0.3	2.358	2.789	2.72	2.9	- 6.2
		6200	2.00	0.305	2.23	0.342	1.928	2.139	2.1	2.32	- 9.5
		3050	1.386	0.332	1.65	0.394	1.307	1.557	1.517	1.59	- 4.6
8.4	8.4	37000	2.82	0.232	3.35	0.272	2.792	3.332	3.204	3.47	- 7.7
		23300	2.65	0.248	3.08	0.29	2.62	3.045	2.94	3.02	- 2.6
		12400	2.32	0.27	2.7	0.31	2.288	2.663	2.57	2.616	- 1.8
15.5	15.5	3760	1.68	0.332	1.83	0.373	1.659	1.806	1.787	1.77	+ 1.0

a. The experimental fluid was air for L/H = 8.4 and 15.5, otherwise silicone oil (Pr>4000). The predictions are based on calculations for Pr=10.

b. from Ozoe et al. [9]; others from Ozoe et al. [10].

Table 6 Computed and extrapolated Nusselt numbers for cubical regions with different boundary conditions (Ra=4000, Pr=10).

Type	X=0 wall	X=1 wall	Y=0 wall	Y=1 wall	Nu ΔZ=0.1	Nu ΔZ→0
A	R	F	R	F	1.6534	1.473
B	F	F	R	F	1.8394	1.642
C	R	F	F	F	1.9243	1.723
D	F	F	F	F	2.1244	1.908
E	R	R	R	F	1.4607	1.300
F	R	R	R	R	1.1425	1.060